International Journal of Nanomedicine

Dovepress
open access to scientific and medical research

Open Access Full Text Article

ORIGINAL RESEARCH

Enhanced antifungal activity of voriconazole-loaded nanostructured lipid carriers against *Candida albicans* with a dimorphic switching model

This article was published in the following Dove Press journal:
International Journal of Nanomedicine
26 September 2017
Number of times this article has been viewed

Baocheng Tian[1]
Qi Yan[1]
Juan Wang[1]
Chen Ding[2]
Sixiang Sai[1]

[1]School of Pharmacy, Binzhou Medical University, Yantai, [2]College of Life and Health Science, Northeastern University, Shenyang, People's Republic of China

Abstract: *Candida* commonly adheres to implanted medical devices and forms biofilms. Due to the minimal activity of current antifungals against biofilms, new drugs or drug-delivery systems to treat these persistent infections are urgently needed. In the present investigation, voriconazole-loaded nanostructured lipid carriers (Vrc-NLCs) were formulated for enhanced drug-delivery efficiency to *C. albicans* to increase the antifungal activity of Vrc and to improve the treatment of infectious *Candida* diseases. Vrc-NLCs were prepared by a hot-melt, high-pressure homogenization method, and size distribution, ζ-potential, morphology, drug-encapsulation efficiency, drug loading, and physical stability were characterized. The antifungal activity of Vrc-NLCs in vitro was tested during planktonic and biofilm growth in *C. albicans*. The mean particle size of the Vrc-NLCs was 45.62±0.53 nm, and they exhibited spheroid-like morphology, smooth surfaces, and ζ-potential of –0.69±0.03 mV. Encapsulation efficiency and drug loading of Vrc-NLCs were 75.37%±2.65% and 3.77%±0.13%, respectively. Physical stability results revealed that despite the low measured ζ-potential, the dispersion of the Vrc-NLCs was stable during their 3-week storage at 4°C. The minimum inhibitory concentration of Vrc-NLCs was identical to that of Vrc. However, the inhibition rate of Vrc-NLCs at lower concentrations was significantly higher than that of Vrc during planktonic growth in *C. albicans* in yeast-extract peptone dextrose medium. Surprisingly, Vrc-NLCs treatment reduced cell density in biofilm growth in *C. albicans* and induced more switches form hyphal cells to yeast cells compared with Vrc treatment. In conclusion, Vrc-NLCs maintain antifungal activity of Vrc and increase antifungal drug-delivery efficiency to *C. albicans*. Therefore, Vrc-NLCs will greatly contribute to the treatment of infectious diseases caused by *C. albicans*.

Keywords: antifungal activity, *Candida albicans*, voriconazole, nanostructured lipid carriers, biofilms

Introduction

Since the early 1980s, fungi have emerged as major causes of human diseases.[1] *Candida* spp. (members of Ascomycota) are found as part of the normal microflora of human mucosal surfaces, although they can sometimes cause vaginitis, oropharyngeal infections, thrush, or urogenital tract infections by invading the host in multiple ways, such as the urogenital tract, lungs, and other mucosal surfaces.[2] Alterations in host immunity, stress, resident microbiota, and other factors cause *C. albicans* overgrowth.[3] *Candida* infections are especially serious in immunocompromised individuals, such as AIDS patients, patients undergoing anticancer therapies, and transplantation patients receiving immunosuppression therapy, as well as immunocompetent patients with implanted medical devices.[4,5]

Correspondence: Sixiang Sai
School of Pharmacy, Binzhou Medical University, 346 Guanhai Road, Laishan, Yantai, Shandong 264003, People's Republic of China
Tel +86 535 691 3254
Fax +86 535 691 3718
Email sixiang.sai@bzmc.edu.cn

submit your manuscript | www.dovepress.com
Dovepress
http://dx.doi.org/10.2147/IJN.S145695

Azoles, the most widely used antifungal agents, are separated into two subgroups: imidazole and triazole. The triazole subgroup comprises fluconazole, itraconazole (first generation), and the newer agents voriconazole (Vrc) and posaconazole (second generation).[6] Azoles achieve their function by inhibiting the enzyme C14α-demethylase. This mechanism results in the accumulation of toxic methylsterols and causes inhibition of cell growth and replication.[7] The antifungal activity of azoles has been improved, due to the development of second-generation azoles, such as Vrc. Although Vrc is widely used in the treatment of fungal infections, it commonly causes adverse effects as patients undergo prolonged therapy.[8] Most concerning is the increased risk of cutaneous malignancies, primarily squamous-cell carcinoma. Vrc is also involved in phototoxicity, periostitis, hallucinations, encephalopathy, peripheral neuropathy, alopecia, nail changes, hyponatremia, and other adverse effects.[9]

Meanwhile, in order to overcome the treatment of antifungal agents, fungi are also evolving drug resistance during infections in their hosts. One the most commonly recognized types of drug resistance is the ability of fungi to generate resilient biofilms within a host. As polymeric material produced by an extracellular matrix, biofilms promote adherence and protect biofilm cells from environmental insults. This material is also associated with the retention of nutrients, water, and enzymes.[10,11] In *Candida* spp., biofilms show innate resistance to multiple drug classes and are capable of neutralizing antifungal concentrations 1,000-fold higher than those that inhibit nonbiofilm – planktonic cells.[12,13] Failure to treat infections associated with *Candida* biofilms can cause serious consequences, progressing to bloodstream infections and invasive fungal infections with high risks of mortality.[14]

Numerous studies have explored how nanomedicine offers a novel approach against biofilm-associated infections in bacteria. Certain characteristics of nanoparticles can enhance antimicrobial activity. Manipulated nanoparticles can increase biofilm entrance and production of reactive oxygen species.[15] Also, the total surface area of nanoparticles is increased by reducing particle sizes to the nanometer level. The resulting higher frequency of drug contact with bacteria benefits the increase in antibacterial activity.[16] Notably, the controlled drug release from nanocarriers at the infection location retains efficient therapy while minimizing toxicity.[17] Nanoparticles can also protect encapsulated drugs from enzymatic and chemical degradation in vivo. Properties of nanomedicine show that it may be useful for applications against biofilm-associated infections in bacteria.[15] Although the structure of biofilm in fungi is different from bacteria, this enlightens research in nanomedicine against biofilm-associated infection in fungi.

The aim of our present study was to determine whether or not the delivery of azole drugs to *C. albicans* would be enhanced by nanoparticles. Vrc-loaded nanostructured lipid carriers (Vrc-NLCs) were prepared. Physicochemical characteristics, such as particle size, ζ-potential, entrapment efficiency, drug loading, physical stability, and vesicle morphology, were investigated. The antifungal activity of Vrc-NLCs against planktonic cells in *C. albicans* was evaluated. In addition, we also provide evidence of NLCs increasing azole-delivery efficiency to *C. albicans* in biofilm-growth conditions.

Materials and methods

Materials

Vrc and Tween 80 were purchased from Sigma-Aldrich (St Louis, MO, USA). Miglyol 812N (caprylic/capric triglycerides) was kindly gifted by Sasol (Witten, Germany). Gelucire 44/14 and Compritol 888 ATO were supplied by Gattefossé (Lyon, France). Solutol HS 15 was provided by BASF (Ludwigshafen, Germany). High-performance liquid chromatography-grade acetonitrile was purchased from DikmaPure (Beijing, China). The purified water used throughout the experiment was purchased from Wahaha Group (Hangzhou, China). All other chemicals and reagents used in the study were of analytical grade quality or higher.

Preparation of NLCs

Vrc-NLCs were produced using the -melt, high-pressure homogenization as described previously, with modification.[18] Briefly, desired amounts of Compritol 888 ATO (50 mg), Miglyol 812N (50 mg), Gelucire 44/14 (50 mg), and Vrc (20 mg) were accurately weighed, mixed, and melted at ~10°C above the melting point of the solid lipid to obtain a transparent and uniform oil phase. Solutol HS 15 (0.75% w:v) and Tween 80 (0.5% w:v) as surfactants were dissolved in purified water at the same temperature to obtain the aqueous phase. The surfactant solution was dispersed in the melted-lipid phase using an XHF-D high-speed homogenizer (Xinzhi Scientific Biotechnology, Ningbo, China) for 1 minute at 8,000 rpm. Afterward, the primary oil-in-water emulsion was homogenized using a high-pressure homogenizer (Nano DeBEE; BEE International, Easton, MA, USA) under 20,000 psi for three cycles. The obtained dispersion

was cooled immediately in an ice bath for 20 minutes to solidify the lipid matrix and form the Vrc-NLCs.

Physicochemical characterization

Particle size, PDI, and ζ-potential measurement

The mean particle size, polydispersity index (PDI) and ζ-potential of the Vrc-NLCs were measured using Zetasizer Nano ZS90 (Malvern Instruments, Malvern, UK) at 25°C after appropriate dilution with purified water. The average particle size was expressed as intensity mean diameter. All experiments were performed in triplicate.

Morphology of NLCs

Transmission electron microscopy (TEM) was used to determine the morphological characteristics of Vrc-NLCs. Nanoparticle suspensions were diluted appropriately with purified water and placed onto a carbon-coated copper grid, followed by formation of a thin liquid film. After extra droplets had been drained off with filter paper, 1% phosphotungstic acid solution was dropped onto the copper grid for negative staining and dried at room temperature. The samples, ie, a dry film on a grid, were observed with TEM (JEM-1200EX; JEOL, Tokyo, Japan) at an accelerating voltage of 60 kV.

Drug-encapsulation efficiency and drug loading

Entrapment efficiency (EE) and drug loading of Vrc-NLCs were determined by measuring the concentration of free drug (unentrapped) in the external aqueous phase using the ultrafiltration method.[19] Vrc-NLCs (500 µL) that had been diluted appropriately with 0.5 wt% Tween 80 were transferred into an Amicon Ultra-4 centrifugal filter device containing ultrafiltration membranes (molecular weight cutoff 10,000 Da; EMD Millipore, Billerica, MA, USA) and centrifuged at 3,500 rpm for 15 minutes. Then, the obtained solution was filtered through a 0.22 µm polyether sulfone syringe filter, and free-drug content was measured by high-performance liquid chromatography on an Agilent 1260 system with a variable wavelength ultraviolet-visible detector. The entire analysis was carried out at 30°C on a C_{18} reverse-phase column (Zorbax SB-C18, 150×4.6 mm, 5 µm; Agilent Technologies, Santa Clara, CA, USA). The Vrc elution was performed with a mobile phase of acetonitrile:purified water (40:60 v:v) at a flow rate of 1 mL/min, and the detector was set at 256 nm. The EE and drug loading of NLCs were calculated thus:

$$EE\ (\%) = \frac{W_{total} - W_{free}}{W_{total}} \times 100 \quad (1)$$

$$DL\ (\%) = \frac{W_{total} - W_{free}}{W_{lipid\ nanoparticles}} \times 100 \quad (2)$$

where W_{total}, W_{free}, and $W_{lipid\ nanoparticles}$ were the amount of Vrc used in formulation, the analyzed amount of the free drug in the external aqueous phase, and the weight of the lipid nanoparticles, respectively.

Physical stability

To determine the physical stability of the Vrc-NLCs dispersion, changes in particle size and ζ-potential were measured during storage at 4°C.[20]

Strains and media

The wild-type *C. albicans* strain SC5314 was routinely cultured in yeast-extract peptone dextrose (YPD) agar (1% yeast extract, 2% peptone, 2% dextrose, 2% agar) at 30°C. To prepare a standard cell suspension, a single colony was inoculated into YPD medium (1% yeast extract, 2% peptone, 2% dextrose) and incubated overnight at 30°C with agitation at 200 rpm. For antifungal activity in vitro, fungal cells were harvested by centrifugation, washed twice in PBS and resuspended in RPMI 1640 (Thermo Fisher Scientific, Waltham, MA, USA) with 2% glucose and YPD medium to 2×10^5 CFU/mL. For biofilm growth, fungal cells were harvested by centrifugation, washed twice in PBS (pH 7.2) and resuspended with Spider medium (1% nutrient broth, 1% mannitol, 1% K_2PO_4, pH 7.2) to 0.5×10^7 CFU/mL.

In vitro antifungal activity

The antifungal activity of different Vrc formulations was tested in vitro against the *C. albicans* strain (SC5314) following National Committee for Clinical Laboratory Standards (NCCLS) guidelines, as described by Chryssanthou et al.[21] For the tested compound, serial dilutions in the range 0.03–16 µg/mL of Vrc-NLCs were prepared in RPMI 1640 with 2% glucose. Vrc in the identical range was tested to determine its inhibition rate against *C. albicans* SC5314, which was considered a positive control for the antifungal activity assay of Vrc-NLCs. Serial dilutions of the tested compound were dispensed into the wells of rows one to ten in 96-well plates in 100 µL inocula with a multichannel pipette. The control group contained 10^5 CFU/mL *C. albicans* in 200-µL RPMI 1640 with 2% glucose. All plates were incubated for 24 hours at 35°C with no agitation. Optical density at 600 nm (OD_{600}) of each well in the 96-well plates was detected using microplate spectrophotometry (BioTek,

Winooski, VT, USA). The inhibition rate of the tested compound was calculated as the percentage of inhibition in *C. albicans* growth compared to the control (the absence of drug). The antifungal activity test for Vrc-NLCs and Vrc in YPD medium was identical to that in RPMI 1640 with 2% glucose, except that 96-well plates were incubated for 24 hours at 30°C with agitation at 200 rpm. All of the assays were performed in triplicate and repeated at least three times for reproducibility.

Disk-diffusion assays

Disk diffusion assays were performed in a Spider agar plate. Briefly, *C. albicans* SC5314 was inoculated into YPD medium and grown overnight at 30°C with agitation at 200 rpm. The cells were then pelleted, washed twice with PBS (pH 7.2), counted with a hemocytometer, and diluted to approximately 10^7 CFU/mL in Spider medium. The mixture was then diluted to 10^4 CFU/mL. A 100 µL cell culture was poured onto Spider agar thoroughly in 100 mm-diameter petri dishes. Vrc-NLCs of concentrations 4 and 16 µg/mL were chosen for further analysis according to these preliminary results of antifungal activity in vitro. Vrc in 1% dimethyl sulfoxide (DMSO) in identical concentrations was used in the positive-control groups. The negative-control groups were treated with 1% DMSO and Vrc-free NLCs. Tested compounds and solvent controls were pipetted onto 6 mm-diameter filter paper. Plates were incubated at 30°C, and inhibition-zone diameters were measured at 24 hours. Each disk-diffusion assay was performed in triplicate and repeated at least three times for reproducibility. Mean diameters were calculated.

Biofilm growth conditions

Squares of silicone (1.5×1.5 cm) cut from silicone sheets (Cardiovascular Instrument, Wakefield, MA, USA) were washed in water and autoclaved. Prior to biofilm growth, squares were incubated with bovine serum (Sigma-Aldrich) overnight. Squares were then washed with 2 mL PBS buffer to remove residual bovine serum and moved to a new 12-well plate. Strains were grown overnight in YPD medium and diluted in Spider medium to OD_{600} of 0.5. Adhesion inanition of biofilm growth was accomplished by adding 2 mL of this cell suspension to a 12-well plate containing silicon squares and incubating at 37°C for 90 minutes with gentle agitation (100 rpm). After this step, each square was gently washed with PBS and 3 mL of fresh Spider medium added. Biofilms were incubated with gentle agitation on a rotary shaker at 37°C for 24 hours. Fresh Spider medium was prepared in broth tubes containing 0.015, 0.5, 4, 8, and 32 µg/mL Vrc and Vrc-NLCs. Antifungal drug-treatment groups were added to 3 mL Spider medium containing drugs in the 12-well plates individually. Control groups were treated with 3 mL Spider medium containing 1% DMSO and Vrc-free NLCs. All groups were incubated with gentle agitation on a rotary shaker at 37°C for an additional 24 hours. The resulting biofilms were photographed using confocal laser-scanning microscopy (CLSM).

Confocal laser-scanning microscopy

Biofilms were visualized by CLSM as described by Nobile and Mitchell.[22] Biofilms on silicone squares were stained with 25 µg/mL concanavalin A–Alexa Fluor 594 conjugate (Thermo Fisher Scientific) for 45 minutes at 37°C. The liquid was then removed from each well and the silicone squares placed on a 35 mm-diameter glass-bottom petri dish (MatTek, Ashland, MA, USA). Biofilms were observed with CLSM (Leica TCS SPE) equipped with a Plan Neofluar 40× magnification/1.3-numerical aperture (for image acquisition) oil objectives. An HeNe1 laser was used to excite at a 543 nm wavelength. All images were captured by a Leica LSM image browser.

Statistical analysis

Experiments were independently repeated at least three times for reproducibility. Data are expressed as the mean ± SD. Statistical analyses were performed using one-way analysis of variance, followed by post hoc comparisons with Tukey's honest significant difference test (SPSS 19.0; IBM, Armonk, NY, USA). Statistically significant differences were set at $P<0.05$. Antifungal tests of Vrc and Vrc-NLCs in 96-well plates followed NCCLS guidelines, and results are shown in Figure S1.

Results and discussion

Physicochemical characterization

Particle size and ζ-potential of vesicles

NLCs were prepared by hot-melt homogenization. Particle-size determination by photon-correlation spectroscopy demonstrated that the mean particle size of Vrc-NLCs was 45.62±0.53 nm (Figure 1A). Nanoparticles for chemotherapy need to be absorbable into cells at a sufficiently high rate and extent. For nanocarrier systems, it has been proposed that particle size plays a key role in their adhesion to and interaction with biological cells.[23] NLC-particle size would have had a fundamental effect on the drug-release behavior of the Vrc from nanodispersions, as well as the nanoparticle

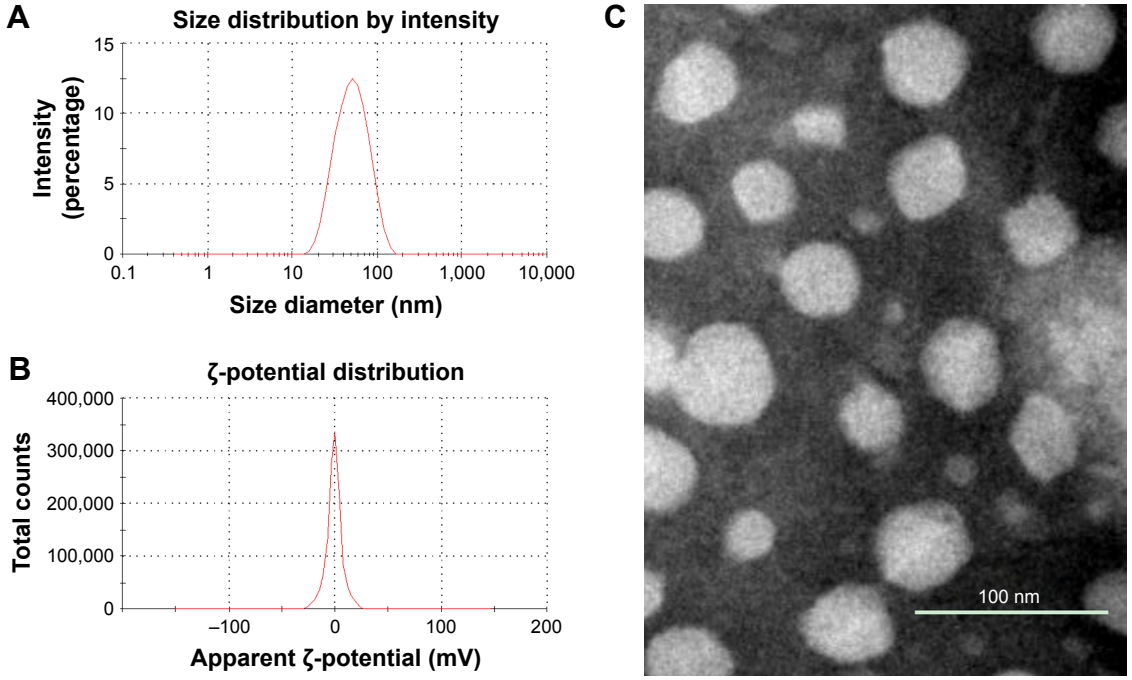

Figure 1 Characterization of NLCs.
Notes: (**A**) Particle-size distribution spectrum of Vrc-NLCs; (**B**) ζ-potential of Vrc-NLCs; (**C**) morphology of Vrc-NLCs determined by TEM.
Abbreviations: NLCs, nanostructured lipid carriers; Vrc, voriconazole; TEM, transmission electron microscopy.

cell-uptake efficiency, which would be directly linked to the antifungal activity of Vrc-NLCs. The Vrc-NLC nanoparticles were in the nanometer range and thus would be expected to have satisfactory drug accumulation in fungal cells. A PDI value of 0.18±0.01 (<0.3) indicated a narrow size distribution that was homogeneous,[24] which is congruent with the unimodal size distribution shown in Figure 1A.

Vrc-NLCs ζ-potentials showed a negative surface charge of –0.69±0.03 mV (Figure 1B). The surface charge is a critical parameter in guaranteeing the physical stability of a nanodispersion.[25] Generally, high absolute ζ-potentials prevent particles from aggregating by electrostatic repulsion among particles with the same electric charge. Absolute ζ-potential >30 mV generally indicates good stability. However, this is valid for low-molecular-weight surfactants and pure electric stabilization, but not for higher-molecular-weight stabilizers, which act mainly by steric stabilization.[26] Although NLCs ζ-potentials were much lower than the critical value of 30 mV, the nonionic surfactant Solutol HS 15 (polyoxyethylene-660-12-hydroxy stearate) employed, with its large hydrophobic segment and long hydrophilic polyethylene glycol chain in the formulation, provided strong steric hindrance to guarantee the long-term stability of the system. Therefore, these nanoparticles would be expected to possess good stability.

Morphology of NLC dispersion

Morphologically, the TEM image in Figure 1C reveals that Vrc-NLCs vesicles showed excellent dispersion and spheroid-like shapes with relatively smooth surfaces. Furthermore, the TEM image shows disaggregated particles of around 50 nm, consistent with the particle-size and ζ-potential measurements with the Zetasizer.

Drug-encapsulation efficiency, drug loading, and physical stability

Vrc was successfully entrapped into NLC nanoparticles. EE and drug loading of Vrc-NLCs were 75.37%±2.65% and 3.77%±0.13%, respectively. This high EE of Vrc into NLCs may have been due to its high partition coefficient in the lipid matrix.

The stability of the Vrc-NLCs dispersion was evaluated for 3 weeks at 4°C. According to the results shown in Table 1,

Table 1 Stability of Vrc-NLCs dispersion at 4°C

Storage	Mean diameter (nm)	ζ-potential (mV)
0	45.62±0.53	0.69±0.03
1 day	43.91±0.79	0.71±0.02
3 weeks	50.2±2.72	0.72±0.03

Note: Data presented as mean ± SD (n=3).
Abbreviations: Vrc, voriconazole; NLCs, nanostructured lipid carriers.

no significant changes in mean vesicle size or ζ-potential were detected. These findings indicated that despite the low measured ζ-potential, the Vrc-NLCs dispersion remained stable during the 3 weeks' storage at 4°C, which can be explained by the steric stabilization provided by the surfactant used.

Antifungal activity in vitro

In order to determine the antifungal activity of Vrc-NLCs, an in vitro antifungal activity test was performed. The test followed the NCCLS guidelines. The results (Figure S1) showed that the minimum inhibitory concentration of Vrc-NLCs was 0.015 μg/mL, identical to that of Vrc, which suggests that Vrc preserves its activity even when it is being loaded in NLCs. Moreover, the increase in concentration of Vrc-NLCs slightly affected *C. albicans* growth in RPMI 1640 with 2% glucose, similar to Vrc. Since endocytosis is an active transport process and influences RPMI 1640 with respect to microorganism growth, the inhibition rate of *C. albicans* in response to Vrc-NLCs was then determined in the YPD medium.

Results are summarized in Figure 2. The inhibition rate of the Vrc-NLCs was dependent on concentration. In groups treated with 8 μg/mL, 4 μg/mL, and 2 μg/mL test component, the inhibition rate of Vrc-NLCs was approximately 8% higher than that of Vrc. In groups treated with 1 μg/mL, 0.5 μg/mL, 0.25 μg/mL, and 0.125 μg/mL test component, the inhibition rate of Vrc-NLCs was slightly higher (approximately 3%) than that of Vrc. In groups treated with 0.06 μg/mL, 0.03 μg/mL, and 0.015 μg/mL test component, the inhibition rate of Vrc-NLCs was significantly higher than that of Vrc. The difference between the inhibition rates even reached 20% in groups treated with 0.015 μg/mL test component. These results indicated that the antifungal activity of Vrc-NLCs was moderately higher than that of Vrc in 1% DMSO. Furthermore, the Vrc-free NLCs negatively impacted cell growth in *C. albicans* (data not shown). A previous study has shown that nanocarrier systems do not negatively impact the antifungal activity of Vrc.[27] Therefore, as one lipid-based colloidal formulation, NLCs may contribute to an improvement in antifungal activity against planktonic cells in *C. albicans*. A probable explanation is that the uptake of Vrc-NLCs by endocytosis was faster than that of Vrc by passive diffusion at specific drug concentrations, which generated more Vrc in cytoplasm in *C. albicans*.

To measure the antifungal activity of Vrc-NLCs against *C. albicans* differentially, the disk-diffusion assay was conducted. The diameter of the inhibition zone is shown in Table 2. Clear zones of inhibition in the components tested were obtained. The results revealed that Vrc-NLCs (in 4 μg/mL and 16 μg/mL concentrations) had a clearly larger zone of inhibition compared with Vrc treatment. These results indicated the potential drug-delivery efficacy of

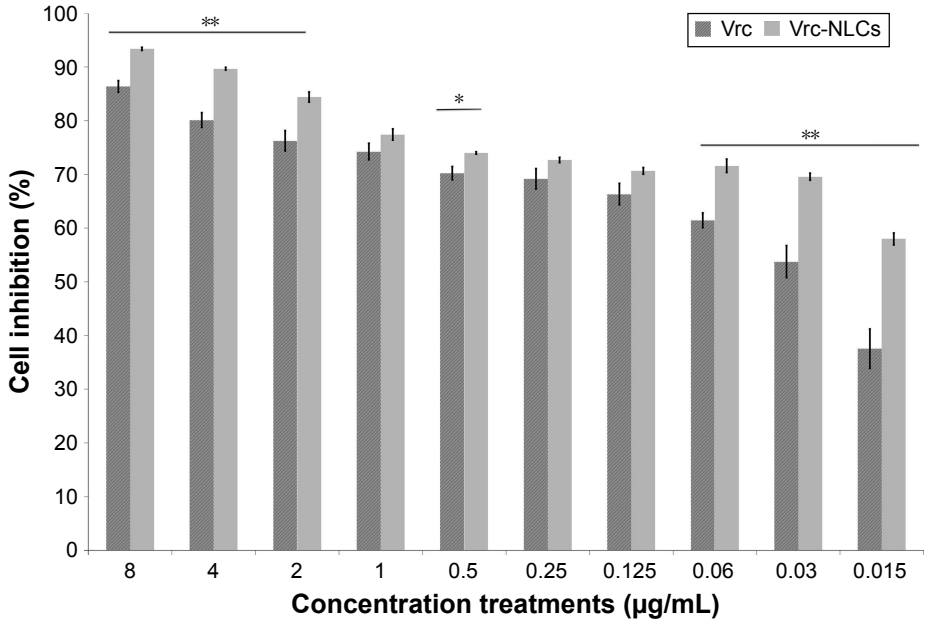

Figure 2 Inhibition rates of Vrc-NLCs against *Candida albicans* in YPD.
Notes: $^{**}P<0.01$; $^{*}P<0.05$. Cells were incubated with different concentrations of Vrc-NLCs and Vrc for 24 hours. Values given in reference to control group, which was cultured without Vrc-NLCs or Vrc. Antifungal activity of Vrc-free NLCs against *C. albicans*, was also tested, showing no activity at the evaluated concentrations. It was considered to have 100% viability in the control group. Vertical bars represent mean ± SD obtained from three experiments for each concentration.
Abbreviations: Vrc, voriconazole; NLCs, nanostructured lipid carriers; YPD, yeast-extract peptone dextrose.

Table 2 *Candida albicans* SC5314-inhibition zones

Formulation	Mean diameter (mm)	Formulation	Mean diameter (mm)
Vrc 4 μg/mL	23.7±1.04*	Vrc-NLCs 4 μg/mL	29±3.97*
Vrc 16 μg/mL	29±1.5*	Vrc-NLCs 16 μg/mL	33.2±1.53*
DMSO control	0	DMSO control	0

Notes: *$P<0.05$. All data presented as mean ± SD (n=3).
Abbreviations: Vrc, voriconazole; NLCs, nanostructured lipid carriers; DMSO, dimethyl sulfoxide.

prepared NLCs, which complemented the in vitro antifungal activity test.

Antifungal activity in biofilm growth

Candida infections frequently involve the formation of biofilms on implanted devices, such as indwelling catheters and prosthetic heart valves.[28] Biofilms of *C. albicans* comprise polysaccharide matrix-enclosed microcolonies of yeasts and hyphae arranged in a bilayer structure.[12,29] The biofilm is able to protect the pathogen from host defenses, antibiotics, and conventional antifungal agents, and offers it a certain amount of spatial stability and autonomy in controlling its own microenvironment.[30] It is still unclear whether the change in drug delivery by NLCs could increase the antifungal activity of Vrc against *C. albicans* during biofilm growth. In this study, we tested antifungal activity in biofilm growth, and the results are shown in Figure 3. Three distinct of *C. albicans* cell types were observed. Yeast cells have a round-to-oval cell morphology that is similar to *Saccharomyces cerevisiae*. By contrast, hyphal cells are thin, tubal cells that resemble segments of a garden hose. Ellipsoid pseudohyphal cells share features of both yeasts and hyphae.[31]

In groups treated with Vrc, increased drug concentration caused dramatic cell-type switching in *C. albicans*. Three types of cells were observed by the depth view of CLSM at 0.05 μg/mL Vrc (Figure 3A), which were similar to the reference group (Figure 3I). The majority of cells were thin, tubal hyphal cells at 4 μg/mL Vrc treatment (Figure 3C), which indicated that *C. albicans* regulated cells switching to hyphal cells in response to moderate antifungal drug treatment. The intense reduction in hyphal cells and increase in yeast cells was observed with 32 μg/mL Vrc treatment (Figure 3G). The results indicated that cell-type switching from hyphal cells to yeast cells was regulated in response to a large amount of Vrc. The overall cell density of *C. albicans* treated with Vrc appeared to be reduced once the drug concentration reached 4 μg/mL. Cell-type switching caused by Vrc-NLCs treatment in *C. albicans* was also observed. However, the number of yeast and pseudohyphal cells in the Vrc-NLC-treatment groups appeared to be more than in the Vrc-treatment groups, since the drug concentration was above 4 μg/mL (Figure 3D). Intriguingly, hyphal cells were not observed in the Vrc-NLC-treatment group, since the drug concentration reached 32 μg/mL (Figure 3H). These results indicated that cell-type switching in *C. albicans* was intensively regulated in response to Vrc-NLCs treatment in comparison to cells undergoing Vrc treatment. Also, cell density at identical drug concentrations in groups treated with Vrc-NLCs was slightly lower than in groups treated with Vrc, which suggested that there was increased antifungal activity of Vrc-NLCs with respect to biofilm cells in *C. albicans*.

In *C. albicans*, morphogenesis is a process by which yeasts, hyphae, and pseudohyphae can either propagate stably as the same cell type or generate other cell types, depending on the local environment. This process has remained the focus of much investigation throughout the decades, due to its importance in aspects of *C. albicans* biology and pathogenicity.[32] It is clear that morphogenesis plays a crucial role in *C. albicans* biofilm development. Hyphae are essential elements in providing the structural integrity and multilayered architecture of mature biofilms.[33] The transition from hyphae cells to yeast cells is a specialized strategy of morphogenetic adaptation that allows for colonization of a host. Morphogenesis requires the fungus to sense and respond to the host environment and is essential for pathogenicity.[34] Therefore, the 32 μg/mL Vrc treatment resulted in the transition from hyphae cells to yeast cells; this might have been because environmental stress triggered *C. albicans* migration to a new location for survival. Because of their smaller and unicellular cells, yeasts are hypothesized to disseminate within the bloodstream, whereas invasive hyphae are thought to escape the vasculature, penetrate internal organs, and damage the host.[35]

Intriguingly, Vrc-NLCs treatment reduced the cell density of biofilm growth in *C. albicans* compared with Vrc treatment at identical dosages. It is already known that nanoparticles are commonly used as drug carriers by endocytosis.[27] During host colonization, hyphal cells induce their endocytic uptake by upregulated expression of hyphal adhesion proteins (eg, Als3), in order to interact with host epithelial cadherin.[36] It is hypothesized that the accumulation of Vrc in cytoplasm by NLCs was larger than that by passive diffusion during biofilm growth in *C. albicans*. Moreover, in biofilm conditions, the extracellular matrix containing β-1,3 glucan sequesters antifungal drugs (eg, azoles) and prevents the drugs from reaching their cellular targets.[37] This *Candida* biofilm-resistance mechanism might benefit drug delivery by NLCs. Due

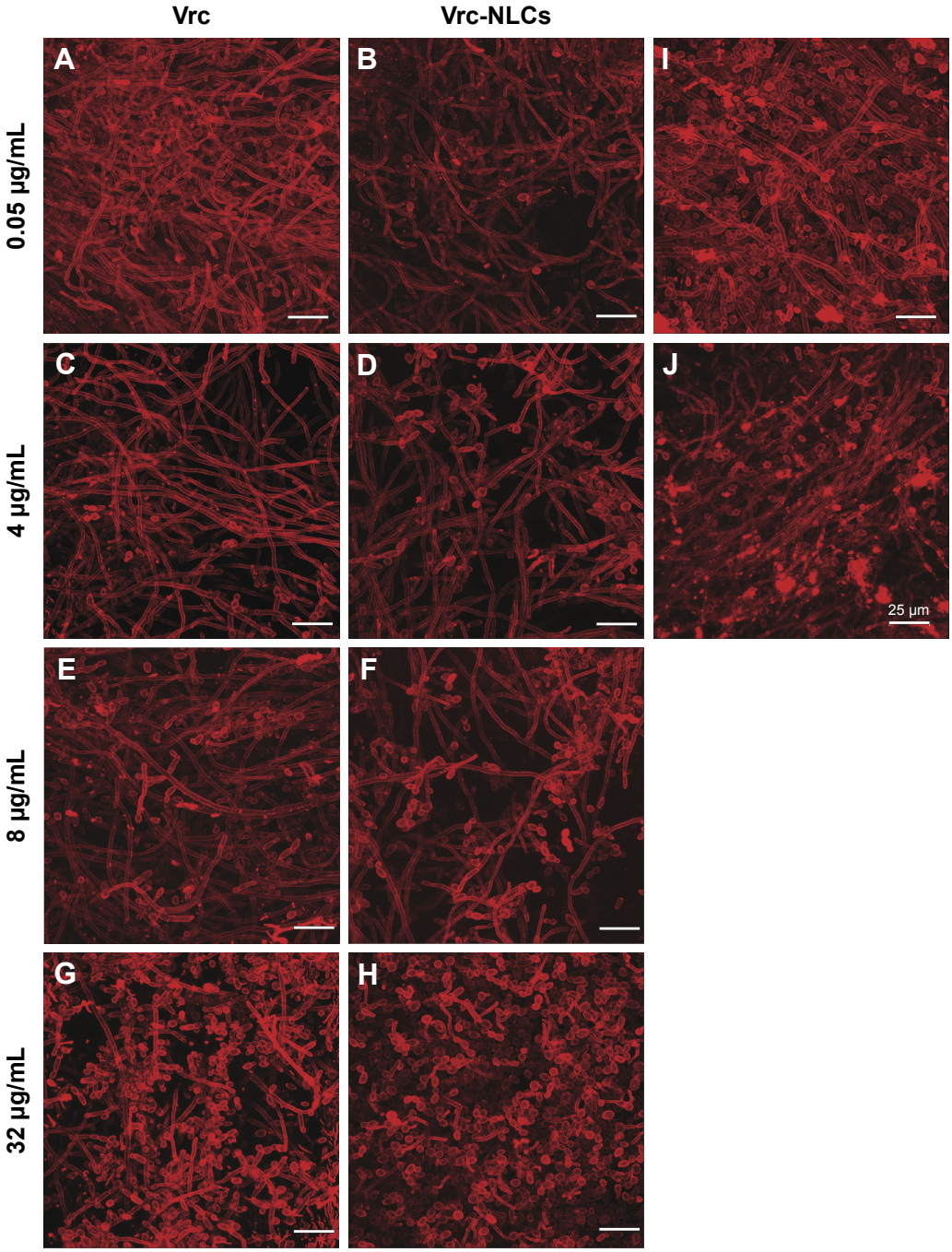

Figure 3 Confocal laser-scanning microscopy showing inhibition of *Candida albicans* biofilm and dimorphic switching by Vrc-NLCs and Vrc.
Notes: (**A**) *C. albicans* biofilm treated with 0.05 μg/mL Vrc; (**B**) *C. albicans* biofilm treated with 0.05 μg/mL Vrc-NLCs; (**C**) *C. albicans* biofilm treated with 4 μg/mL Vrc; (**D**) *C. albicans* biofilm treated with 4 μg/mL Vrc-NLCs; (**E**) *C. albicans* biofilm treated with 8 μg/mL Vrc; (**F**) *C. albicans* biofilm treated with 8 μg/mL Vrc-NLCs; (**G**) *C. albicans* biofilm treated with 32 μg/mL Vrc; (**H**) *C. albicans* biofilm treated with 32 μg/mL Vrc-NLCs; (**I**) *C. albicans* biofilm treated with 1% dimethyl sulfoxide; (**J**) *C. albicans* biofilm treated with Vrc-free NLCs. Bar 25 μm. Magnification 600×.
Abbreviations: Vrc, voriconazole; NLCs, nanostructured lipid carriers.

to the mechanism of morphogenesis in response to antifungal drugs and the characteristics of NLCs in drug delivery, treatment with 32 μg/mL Vrc-NLCs induced hyphal cells switching to yeast cells and pseudohyphal cells. Taken together, the antifungal activity of Vrc-NLCs on biofilm cells in *C. albicans* was increased in comparison with Vrc.

Conclusion

In the present study, we successfully developed Vrc-NLCs for efficient drug delivery. The NLCs were spherical with appropriate particle size and exhibited high EE. The physical stability assay suggested that Vrc-NLCs dispersion was stable during 3 weeks' storage at 4°C. Furthermore, the antifungal

activity of Vrc-NLCs was evaluated against *C. albicans*. During planktonic growth, Vrc-NLCs showed an increased inhibition rate at lower concentrations in comparison with Vrc. This might be explained by increased drug-delivery efficiency of NLCs at specific concentrations. Remarkably, the results indicated that Vrc-NLCs improved antifungal activity against the biofilm state of *C. albicans*. During biofilm growth, hyphal cells raise the production of biofilm. The key feature of mature biofilms is the production of an extracellular matrix, which promotes adherence and protects cells from antifungals. Consequently, it was hypothesized that NLCs dramatically improved drug delivery to penetrate the extracellular matrix in hyphal cells and regular cell-wall structures in yeast cells. This unique advantage of NLCs benefits antifungal activity of Vrc against *C. albicans*. Vrc-NLCs have superior prospects in the field of antifungals, and further studies of their antifungal activity in vivo should be encouraged.

Acknowledgments

This work was financially supported by the National Natural Science Foundation of China (81501784, 31300974, and 31401258), the Shandong Provincial Natural Science Foundation (ZR2014HQ069), the Fundamental Research Funds for Central Universities of China (N142005001), and the Project of Shandong Province Higher Educational Science and Technology Program (J14LM51).

Disclosure

The authors report no conflicts of interest in this work.

References

1. Pfaller MA, Diekema DJ. Epidemiology of invasive candidiasis: a persistent public health problem. *Clin Microbiol Rev*. 2007;20(1):133–163.
2. Hazen KC. New and emerging yeast pathogens. *Clin Microbiol Rev*. 1995;8(4):462–478.
3. Nobile CJ, Johnson AD. *Candida albicans* biofilms and human disease. *Annu Rev Microbiol*. 2015;69:71–92.
4. Calderone RA, Fonzi WA. Virulence factors of *Candida albicans*. *Trends Microbiol*. 2001;9(7):327–335.
5. Weig M, Gross U, Mühlschlegel F. Clinical aspects and pathogenesis of *Candida* infection. *Trends Microbiol*. 1998;6(12):468–470.
6. Moudgal V, Sobel J. Antifungals to treat *Candida albicans*. *Expert Opin Pharmacother*. 2010;11(12):2037–2048.
7. Sheehan DJ, Hitchcock CA, Sibley CM. Current and emerging azole antifungal agents. *Clin Microbiol Rev*. 1999;12(1):40–79.
8. Re VL, Carbonari DM, Lewis JD, et al. Oral azole antifungal medications and risk of acute liver injury, overall and by chronic liver disease status. *Am J Med*. 2016;129(3):283–291.
9. Levine MT, Chandrasekar PH. Adverse effects of voriconazole: over a decade of use. *Clin Transplant*. 2016;30(11):1377–1386.
10. Ramage G, Saville SP, Wickes BL, Lopez-Ribot JL. Inhibition of *Candida albicans* biofilm formation by farnesol, a quorum-sensing molecule. *Appl Environ Microbiol*. 2002;68(11):5459–5463.
11. Baillie GS, Douglas LJ. Matrix polymers of *Candida* biofilms and their possible role in biofilm resistance to antifungal agents. *J Antimicrob Chemother*. 2000;46(3):397–403.
12. Douglas LJ. *Candida* biofilms and their role in infection. *Trends Microbiol*. 2003;11(1):30–36.
13. Donlan RM, Costerton JW. Biofilms: survival mechanisms of clinically relevant microorganisms. *Clin Microbiol Rev*. 2002;15(2):167–193.
14. Ramage G, Mowat E, Jones B, Williams C, Lopez-Ribot J. Our current understanding of fungal biofilms. *Crit Rev Microbiol*. 2009;35(4):340–355.
15. Taylor E, Webster TJ. Reducing infections through nanotechnology and nanoparticles. *Int J Nanomedicine*. 2011;6:1463–1473.
16. Baker C, Pradhan A, Pakstis L, Pochan DJ, Shah SI. Synthesis and antibacterial properties of silver nanoparticles. *J Nanosci Nanotechnol*. 2005;5(2):244–249.
17. Hindi KM, Ditto AJ, Panzner MJ, et al. The antimicrobial efficacy of sustained release silver-carbene complex-loaded L-tyrosine polyphosphate nanoparticles: characterization, in vitro and in vivo studies. *Biomaterials*. 2009;30(22):3771–3779.
18. Shangguan M, Qi J, Lu Y, Wu W. Comparison of the oral bioavailability of silymarin-loaded lipid nanoparticles with their artificial lipolysate counterparts: implications on the contribution of integral structure. *Int J Pharm*. 2015;489(1–2):195–202.
19. Sütő B, Berko S, Kozma G, et al. Development of ibuprofen-loaded nanostructured lipid carrier-based gels: characterization and investigation of in vitro and in vivo penetration through the skin. *Int J Nanomedicine*. 2016;11:1201–1212.
20. Alomrani AH, Shazly GA, Amara AA, Badran MM. Itraconazole-hydroxypropyl-β-cyclodextrin loaded deformable liposomes: in vitro skin penetration studies and antifungal efficacy using *Candida albicans* as model. *Colloids Surf B Biointerfaces*. 2014;121:74–81.
21. Chryssanthou E, Cuenca-Estrella M. Comparison of the Antifungal Susceptibility Testing Subcommittee of the European Committee on Antibiotic Susceptibility Testing proposed standard and the E-test with the NCCLS broth microdilution method for voriconazole and caspofungin susceptibility testing of yeast species. *J Clin Microbiol*. 2002;40(10):3841–3844.
22. Nobile CJ, Mitchell AP. Regulation of cell-surface genes and biofilm formation by the C. albicans transcription factor Bcr1p. *Curr Biol*. 2005;15(12):1150–1155.
23. Win KY, Feng SS. Effects of particle size and surface coating on cellular uptake of polymeric nanoparticles for oral delivery of anticancer drugs. *Biomaterials*. 2005;26(15):2713–2722.
24. Luan J, Zheng F, Yang X, Yu A, Zhai G. Nanostructured lipid carriers for oral delivery of baicalin: in vitro and in vivo evaluation. *Colloids Surf A Physicochem Eng Asp*. 2015;466:154–159.
25. Das S, Ng WK, Kanaujia P, Kim S, Tan RB. Formulation design, preparation and physicochemical characterizations of solid lipid nanoparticles containing a hydrophobic drug: effects of process variables. *Colloids Surf B Biointerfaces*. 2011;88(1):483–489.
26. Mishra PR, al Shaal L, Müller RH, Keck CM. Production and characterization of hesperetin nanosuspensions for dermal delivery. *Int J Pharm*. 2009;371(1–2):182–189.
27. Aljuffali IA, Huang CH, Fang JY. Nanomedical strategies for targeting skin microbiomes. *Curr Drug Metab*. 2015;16(4):255–271.
28. Andes D, Nett J, Oschel P, Albrecht R, Marchillo K, Pitula A. Development and characterization of an in vivo central venous catheter *Candida albicans* biofilm model. *Infect Immun*. 2004;72(10):6023–6031.
29. Soll DR. *Candida* biofilms: is adhesion sexy? *Curr Biol*. 2008;18(16):R717–R720.
30. De Sordi L, Mühlschlegel FA. Quorum sensing and fungal-bacterial interactions in *Candida albicans*: a communicative network regulating microbial coexistence and virulence. *FEMS Yeast Res*. 2009;9(7):990–999.
31. Sudbery P, Gow N, Berman J. The distinct morphogenic states of *Candida albicans*. *Trends Microbiol*. 2004;12(7):317–324.
32. Brand A, Gow NA. Mechanisms of hypha orientation of fungi. *Curr Opin Microbiol*. 2009;12(4):350–357.

33. Baillie GS, Douglas LJ. Role of dimorphism in the development of *Candida albicans* biofilms. *J Med Microbiol*. 1999;48(7):671–679.
34. Boyce KJ, Andrianopoulos A. Fungal dimorphism: the switch from hyphae to yeast is a specialized morphogenetic adaptation allowing colonization of a host. *FEMS Microbiol Rev*. 2015;39(6):797–811.
35. Noble SM, Gianetti BA, Witchley JN. *Candida albicans* cell-type switching and functional plasticity in the mammalian host. *Nat Rev Microbiol*. 2017;15(2):96–108.
36. Phan QT, Myers CL, Fu Y, et al. Als3 is a *Candida albicans* invasin that binds to cadherins and induces endocytosis by host cells. *PLoS Biol*. 2007;5(3):e64.
37. Nett J, Lincoln L, Marchillo K, et al. Putative role of β-1,3 glucans in *Candida albicans* biofilm resistance. *Antimicrob Agents Chemother*. 2007;51(2):510–520.

Supplementary material

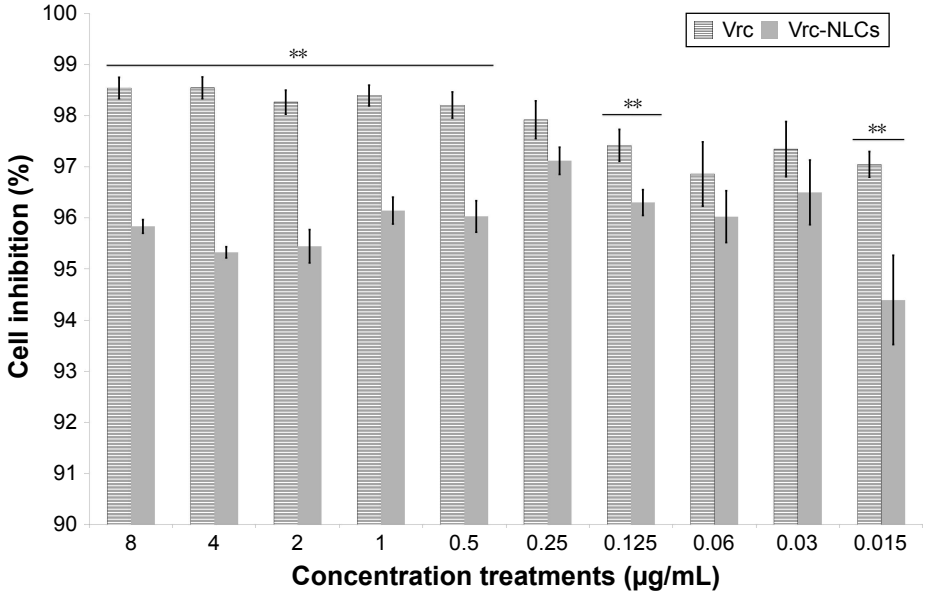

Figure S1 Inhibition rates of Vrc-NLCs against *Candida albicans* in RPMI 1640.
Notes: $^{**}P<0.01$. Cells were incubated with different concentrations of Vrc-NLCs and Vrc for 24 hours at 35°C. Values given in reference to control group, which was cultured without Vrc-NLCs or Vrc. Vertical bars represent mean ± SD obtained from three experiments for each concentration.
Abbreviations: Vrc, voriconazole; NLCs, nanostructured lipid carriers.